3D MEMS IN STANDARD PROCESSES: FABRICATION, QUALITY ASSURANCE, AND NOVEL MEASUREMENT MICROSTRUCTURES

Gisela Lin, Russell A. Lawton
Jet Propulsion Laboratory
4800 Oak Grove Drive, MS 302-231
Pasadena, CA 91109-8099 USA

Abstract

Three-dimensional MEMS microsystems that are commercially fabricated require minimal post-processing and are easily integrated with CMOS signal processing electronics. Measurements to evaluate the fabrication process (such as cross-sectional imaging and device performance characterization) provide much needed feedback in terms of reliability and quality assurance. MEMS technology is bringing a new class of microscale measurements to fruition. The relatively small size of MEMS microsystems offers the potential for higher fidelity recordings compared to macrosize counterparts, as illustrated in the measurement of muscle cell forces.

Introduction

Micro-electromechanical systems (MEMS) technology provides a relatively new, inexpensive way to make sensors. Chemical, inertial, thermal, and pressure sensors have been miniaturized using silicon-based integrated circuit fabrication techniques. The sensing components of these devices are generally two-dimensional in shape and utilize the electrical and mechanical properties of bulk silicon and deposited thin films [1]. Three-dimensional structures have been demonstrated using folded polymers or precision assembly of 2D structures, but these types of structures usually require custom processing [2] [3]. By taking advantage of commercial fabrication facilities, investigators can focus on design. Sophisticated devices can be made without having to own an expensive fabrication facility. Also, several design iterations can be made inexpensively in a relatively short time while avoiding the problems of custom processing.

Fabrication

Typically, a device is first designed with a Computer Aided Design (CAD) tool. There are many tools currently available from companies such as MEMSCAP Inc. [4] which allow the user to design a MEMS device, optimize it, simulate it, verify its functionality, and generate its layout. This layout is then sent to the foundry. After the chip is fabricated, a maskless post-processing release step is performed where "sacrificial" layers are etched away, allowing the structural layers to move and rotate. Following release, the devices are assembled and tested.

Two commercially available processes will be highlighted in this paper One is a polysilicon surface micromachining process (MUMPs™) [5] while the other is a standard 2μm

Complementary Metal-Oxide-Semiconductor (CMOS) process [6]. Both processes can be used to create complex three-dimensional MEMS microstructures. The layer stack of the MEMS-based process is shown in Figure 1. This process offers two structural layers of polysilicon (poly1 and poly2) and two sacrificial layers of silicon dioxide (oxide1 and oxide2). The poly0 layer is used as an electrical ground plane rather than a structural layer. Patterning the layers is done via photolithography and reactive ion etching.
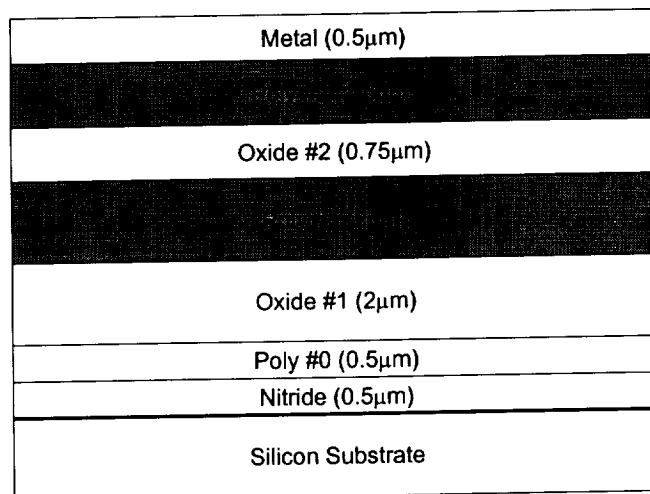

Figure 1. *MUMPs™ layer stack [5]. Poly1 and poly2 are structural polysilicon layers, while the oxides are sacrificial layers in that they do not appear in the final structure. Poly0 is used as a ground plane and the nitride is used for electric isolation. Metal layer on top (gold) is for optional contact metalization.*

The oxide layers are considered "sacrificial" layers because they do not appear in the final structure. When the chips come back from the foundry, the oxide is etched, freeing the polysilicon layers and allowing them to move. By connecting poly1 to poly2 (or poly2 to the substrate) in strategic locations, a variety of hinges can be constructed that allow plates of polysilicon to rotate out of the plane of the wafer and with respect to each other [7]. The required etchant is liquid 49% hydrofluoric acid (HF) which has very high selectivity for oxide over silicon and polysilicon. Proper drying of the chip after release is important to reduce the possibility of the polysilicon structures sticking to the substrate (stiction). There are many methods to dry the chips, such as supercritical carbon dioxide drying [8].

Although this MEMS-based process has much to offer, it does not currently support on-chip integrated electronics. Thus, a standard 2μm CMOS process is used to create 3D MEMS structures with on-chip sensing electronics [6]. The available layer stack for this process is shown in Figure 2. In this process Metal-Oxide-Semiconductor Field Effect Transistors (MOSFETs) are fabricated along with MEMS microstructures. All lithography and thin film patterning was performed during this process.
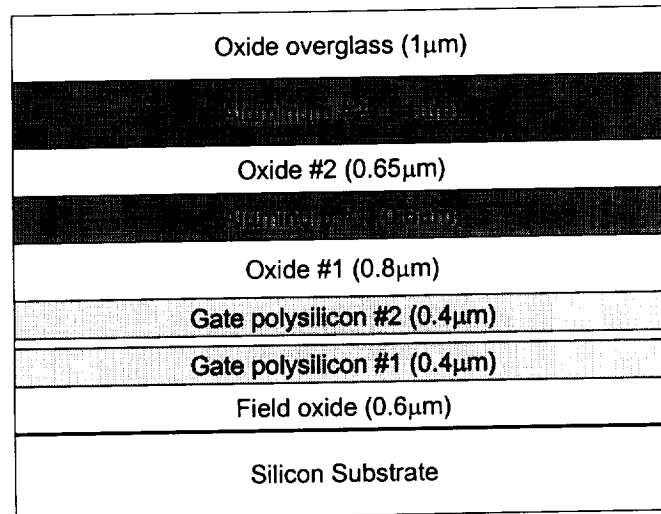
Figure 2. *CMOS layer stack. 500Å of thermally grown SiO$_2$ is located between the polysilicon layers.*

When the chips come back from the CMOS foundry, they require a single unmasked etch. In this case, the primary structural material is silicon dioxide and the silicon substrate is the sacrificial material. "Vias" are holes patterned in the oxide layers by which layers of polysilicon and metal are connected to the substrate and/or each other. Etch windows are created by patterning successive vias on top of each other, thereby leaving the substrate exposed. This exposed silicon can then be etched to undercut and release the oxide microstructures and does not require a mask since the etching areas are already patterned at the foundry. The only parameters are choice of silicon etchant, etch temperature, and etching time.

Ideally, the oxide microstructures can be released using any wet silicon etchant such as TMAH or KOH. However, due to the delicacy of most microstructures, a dry-phase etchant such as XeF$_2$ is preferred [9]. This isotropic gas-phase etchant offers high selectivity toward silicon dioxide and aluminum, and it eliminates any liquid meniscus forces or bubbles that can damage the microstructures. Freestanding aluminum beams can be created which act as mechanical hinges as well as electrical interconnects [10].

Quality Assurance Measurements

Process integrity is essential to successful MEMS device fabrication and can be assessed by several key metrics. An accurate measurement of layer thicknesses and profiles is extremely important. Traditionally, device cross-section images are obtained by cleaving the wafer through the device, mounting the wafer in a specially designed chip holder, and imaging the cleaved area using a scanning electron microscope (SEM). This procedure can be quite destructive and hundreds of devices may be sacrificed. With a focussed ion beam (FIB) system, these

measurements can be taken without the need for special chip holders or wafer cleaving [11]. This system uses a gallium ion beam to mill a portion of the device and an electron beam to produce a high resolution image of the device cross-section.

Images were obtained from identically fabricated unreleased chips from two non-commercial fabrication facilities running surface micromachining processes. As shown in Figure 3, the cross-sections are dramatically different. The oxide in Figure 3(a) has sloping sidewalls compared to that in Figure 3(b). Furthermore, the oxide in Figure 3(b) was not completely etched. The thin sheet of oxide separating the first and second layers of polysilicon will cause second layer to detach from the first layer during the release etch (a catastrophic failure). These results may be due to different material properties of the oxides or differences in the RIE hardware and/or RIE plasma chemistries. This type of information is required for adequate process quality control.
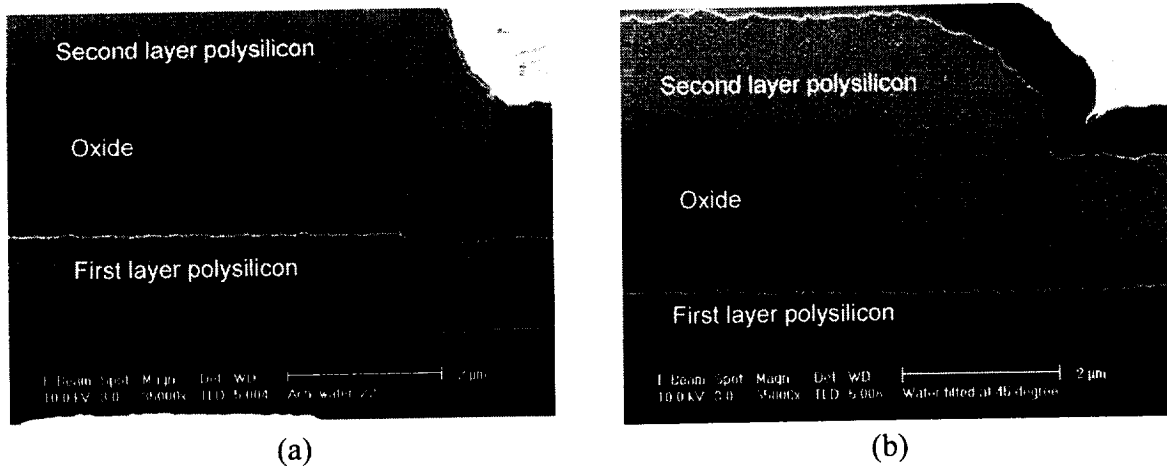

(a)   (b)

Figure 3. *FIB/SEM cross-sections from identically fabricated chips from two separate non-commercial fabrication facilities.*

Slight variations in the processing parameters will also result in microstructures with different performance characteristics. For example, suspension beam width variations in comb drive test structures fabricated at Cronos Integrated Microsystems resulted in variations in resonant frequency Figure 4 [5] [12]. In a single fabrication run, beam width varied by 200nm across an entire wafer, presumably due to variations in line exposures during photolithography and/or variations in RIE etching profiles. Since the lateral resonant frequency goes with suspension beam width to the 3/2 power [12], the resulting devices vary in resonant frequency by at most 3kHz, which may or may not be detrimental depending on the device application.

MEMS device performance characteristics can also be affected by the release method used. A recent study at JPL involved FIB and scanning laser vibrometer analysis of the comb drive test structures released by three different methods (liquid HF, low power ultrasound in

liquid HF, and vapor HF) [13]. It was found that the out-of-plane motion was minimally affected in the vapor released chip, but that of the liquid released chips was either partially hindered or totally blocked due to stiction. This information is crucial to fabrication process optimization and reliability.
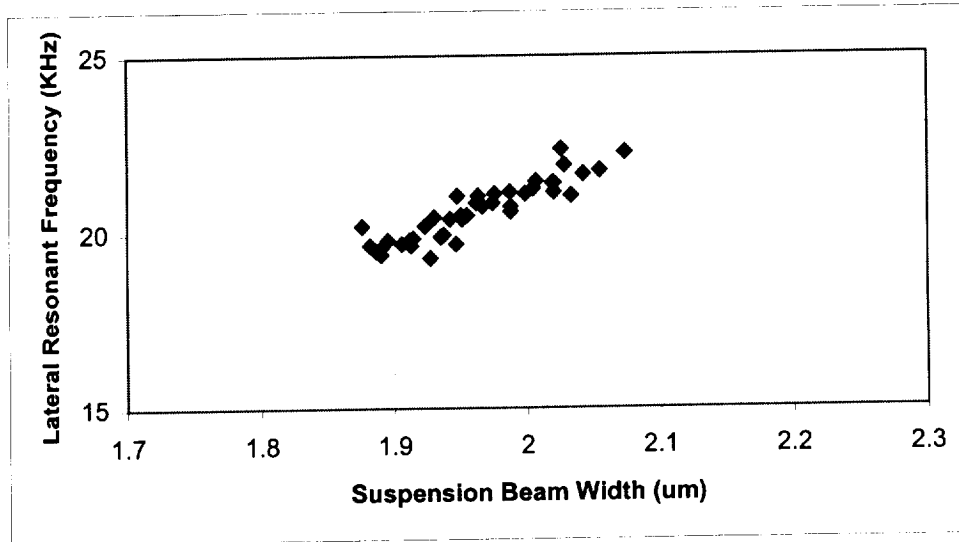

Figure 4. *Variation in resonant frequency of as a result of variations in beam width for the MUMPs™ 17 fabrication run.*

Besides device performance and cross-sectional imaging, there are numerous other aspects of reliability and quality assurance such as *in-situ* process monitoring during deposition/layer growth, residual stress measurements, and the use of custom integrated MEMS testing benches for more complicated analyses [14]. Since material properties and (micro)geometries are subject to manufacturing variations, it is necessary to establish these parameters (or at least a sufficient number of indicators) for each wafer or fabrication facility. To this end each wafer needs to incorporate one or more test structures, on which specialized characterization tests are performed routinely to characterize the particular fabrication process. This data is then put into a solid mechanics analysis that then produces a reliability estimate. It is anticipated that all commercial foundries will perform these standardized measurements and supply the data to the customer along with the MEMS chips.

Novel Measurement Microstructures

MEMS technology allows investigators to create miniature sensors and transducers that open the doors to a new class of microscale measurements. MEMS are currently used to measure pressure, acceleration, material strain, fluid flow, surface profiles, and chemical compounds [1]. The small size and high sensitivity of many MEMS devices are distinct advantages over macroscale counterparts.

To illustrate this point, we focus on the use of MEMS to measure force generated by muscle cells. Mammalian heart cells are roughly 2-dimensional in shape, 20 - 30μm wide and 100 - 150μm long. Thus, the size of the cell matches the size of typical MEMS devices. Macro transducers are massive compared to the size of a single heart cell and are inherently limited in frequency response and sensitivity. Glass pipettes are required to enter the solution meniscus to contact the cell and are subject to surface tension forces which complicate the measurement.

A miniature, highly sensitive, fully submersible MEMS force transducer offers the possibility of higher frequency measurements, which are important to the understanding and quantitative analysis of the molecular mechanisms of cellular contraction. To this end, MEMS heart cell force transducers were designed using the MEMS-based and CMOS fabrication facilities [5] [6]. In the MEMS-based process, polysilicon clamps were created by utilizing spring locks and scissor hinges (Figure 5) [7].
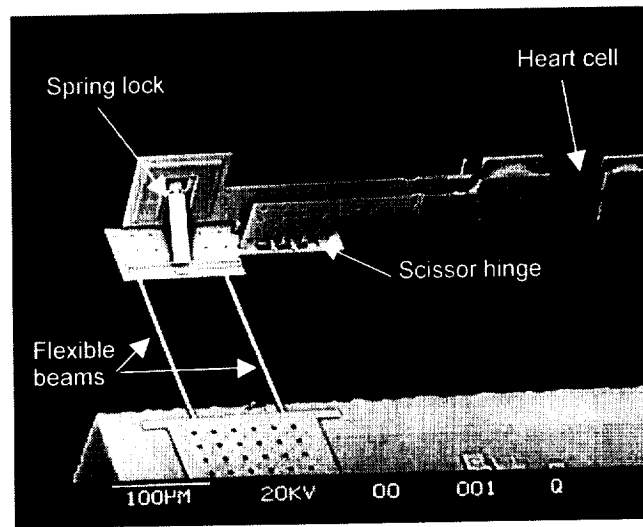

Figure 5. *Close-up of one of two polysilicon clamps holding each end of a heart cell. Vertical plates are attached to a movable shuttle. Scissor hinges allow the vertical plates to rotate with respect to each other and translate in response to the cell's contraction. A spring lock supports the back vertical plate at 90°. A cell is glued between the clamps using a silicone sealant. Dimensions of each beam are 200 × 4 × 2 μm³. [15].*

When the cell contracts, the beams bend and the amount of cell shortening is optically determined. Force is estimated by taking half the total shortening and multiplying this value by the calibrated spring constant in the beams. Force data from rat heart cells were recorded during their response to activation solutions with various levels of calcium ion. The average maximal force over seven cells was F_{max} = 12.6 ± 4.66 μN [15]. These forces were comparable to those measured by other groups studying the contractile characteristics of rat heart cells [17] [18].

Beam calibration was performed separately by hanging glass weights off the tips of the beams and measuring the resulting downward deflection. The weights were made from thin glass

tubing and ranged from 0.7 - 2.5 ± 0.1mg (1mg ≈ 10μN) [16]. The weight of the polysilicon clamp at the end of the beams was negligible compared to the calibration weights. A horizontal optical axis microscope system was used to view the device as well as record the vertical deflection of the beams before and after the weight was applied. The average spring constant over five samples was 1.47 ± 0.36 N/m.

Despite the success of the polysilicon version, it required a visual deflection readout which was not optimal due to the necessary high beam compliance and finite video image resolution. Therefore, a CMOS version was pursued that incorporated on-chip strain gauges and amplification electronics to achieve a voltage readout. As shown in Figure 6, the cell is held between two silicon dioxide clamps. When the cell contracts, it bends the sensor beam and activates the piezoresistive polysilicon strain gauge (the opposite beam is immobilized during the experiment). This strain gauge is completely encased in oxide and functions as the variable resistor in a Wheatstone bridge connected to an on-chip amplifier. The signal is further amplified and filtered off-chip. The clamps and beams are part of an entire 3D microstructure that was undercut in XeF_2 and flipped over the edge of the wafer using aluminum hinges [10] [19].
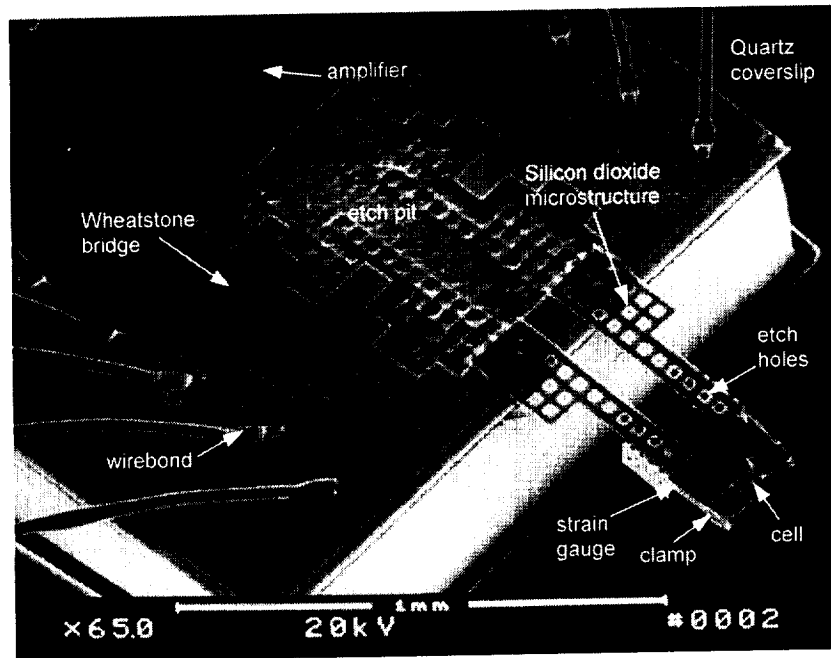

Figure 6. *SEM photo of the device, without encapsulation. A quartz coverslip is attached to the chip which comprises part of the package as well as allows transmitted light illumination of the cell. The XeF_2-etched pit is clearly visible once the microstructure is flipped over the edge of the wafer. The base of the lower beam contains a piezoresistor connected to the rest of a Wheatstone bridge via the aluminum hinges. Gold wirebonds transfer the electrical signals on and off the chip. Dimensions of each beam are $100 \times 20 \times 3.05 \mu m^3$ [20].*

Real time cellular force traces were obtained from this device. A typical force record from a living rat heart cell resulting from calcium activation solution infusion is shown in Figure

7. Upon solution exchange, a transient spike arose from the initial burst of fluid deflecting the sensor beam. Fluid flow produced a shift in DC voltage level due to mechanical force on the beam. The delay in activation/relaxation following the introduction of a new solution was due to its transit time in the experimental chamber and diffusion in the cell. The fluctuation in the record was caused by fluid currents during solution exchange. Clearly shown is the DC voltage level shift due to the cell's force on the sensor beam. Using the calibrated spring constant of the sensor beam, this voltage shift corresponded to approximately 7μN of force. Typically, contractile forces in the 4 - 9μN range were measured.
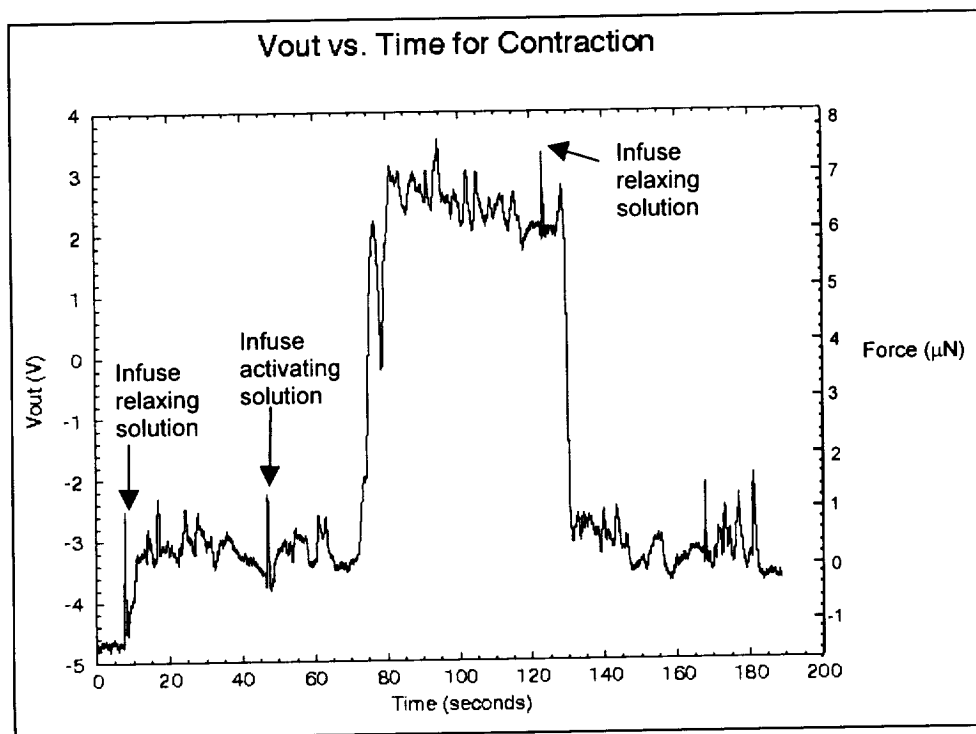

Figure 7. *Trace recorded via data acquisition during cell contraction in response to a calcium activating solution and during relaxation in response to a relaxing solution. The ripples in the data are due to fluid currents during solution exchange.*

The sensor beam containing the strain gauge was separately calibrated using a standard "macro" force transducer, the Cambridge 406A (Cambridge Technologies, Watertown, MA 02172). The Cambridge transducer was used to apply a known force to the beam by directly interfacing its glass pipette tip to the end of the MEMS transducer beam. The change in output voltage of both the Cambridge and the MEMS force transducers were recorded simultaneously for various amounts of applied force. The Cambridge force transducer was calibrated separately by hanging wires of known weights off the force transducer. Its calibrated response was 13mV/μN and was linear.

Using this factor, the change in Cambridge output voltage could be converted to applied force and plotted versus the corresponding change produced in the MEMS system output voltage. The resulting ΔV_{out} vs. force curve was linear with a small amount of scatter. One source of the scatter was slippage or variation in contact interface between the polished and rounded Cambridge pipette tip and the MEMS beam. Averaging over eight devices, the MEMS system response was 0.81 ± 0.16 V/μN. Dividing by the gain of the off-chip amplifier (511), the on-chip system response was 1.6 ± 0.31 mV/μN [20].

In a separate experiment, each beam was deflected with a metal probe in air, and the corresponding change in MEMS system output voltage (V_{out}) was recorded. By dividing the slope of the best fit line in the ΔV_{out} vs. deflection curve by the slope of the ΔV_{out} vs. force curve, an estimate of the spring constant of the beam for each device could be obtained. Averaging over eight devices, the calibrated spring constant of the beam was 2.8 ± 0.42 N/m [20].

To determine the mechanical bandwidth of the sensor beam, the beam was deflected approximately 10μm and quickly released. The release was done by delivering a step voltage to an external piezoelectric perturbator. The perturbator is an inexpensive piezoelectric membrane with a 4" long needle attached to it. A tungsten needle probe which contacts the beam was attached to the end of this needle. This probe was used to initially deflect and preload the beam at the beam tip. The beam was released when the step voltage caused the probe to quickly move forward and "flick" the beam. Using this method, the mechanical bandwidth is approximately 30.3kHz in air and 13.3kHz in water [20]. Compared to the 100s of hertz attainable by most macroscale force transducers, the MEMS device offers a much higher frequency response.

Conclusions

We present methods to fabricate 3D MEMS in two commercially available processes. One is a MEMS-based process in which the primary structural material is polysilicon, the other is a 2μm CMOS process in which the primary structural material is silicon dioxide. The CMOS process offers the compatibility of on-chip electronics integration with the MEMS microstructures. Measurements to evaluate the process integrity are crucial, as slight variations will result in devices that may have undesirable characteristics. However, MEMS microsystems can be created that allow new, high fidelity microscale measurements to be made. A prime example is the measurement of single heart cell forces, where the size of the MEMS measurement system is on the order of the cell's size. This advantage allows higher frequency real time recording of force development compared to macrosize force transducers.

Acknowledgement

References

[1] Gregory T. A. Kovacs, *Micromachined Transducers Sourcebook*, WCB/McDraw-Hill, Boston, 1998.

[2] K. Suzuki, I. Shimoyama, and H. Muira, "Insect-Model Based Microrobot with Elastic Hinges," *Journal of Microelectromechanical Systems*, vol. 3, no. 1, March 1994.

[3] A. C. Hoogerwerf, K. D. Wise, "A Three-dimensional Neural Recording Array," *Transducers '91*, San Francisco, California, June 24 - 27, pp. 120-123, 1991.

[4] MEMSCAP, Inc., P.O. Box 14306, Research Triangle Park, North Carolina 27709 USA. http://memscap.e-sip.com/

[5] Cronos Integrated Microsystems, Inc., 3000 Aerial Center Pkwy, Suite 110, Morrisville, NC 27560, USA. http://www.memsrus.com/

[6] MOSIS foundry service using Orbit Semiconductor's 2μm CMOS process. USC/Information Sciences Institute, 4676 Admiralty Way, Marina Del Rey, CA 27709. http://www.mosis.org/

[7] K. S. J. Pister, M .W. Judy, S. R. Burgett, and R. S. Fearing, "Microfabricated Hinges," *Sensors and Actuators (A)*, vol. 33, no. 3, pp. 249 - 256, 1992.

[8] G. T. Mulhern, D. S. Soane, and R. T. Howe, "Supercritical Carbon Dioxide Drying of Microstructures," Transducers '93, Yokahama, Japan, June 7 - 10, 1993, pp. 296-299.

[9] P. B. Chu, J. T. Chen, R. Yeh, G. Lin, C. P. Huang, B. A. Warneke, and K. S. J. Pister, "Controlled Pulse-Etching with Xenon Difluoride," *Transducers '97*, Chicago, Illinois, pp. 665 - 668, June 16 - 19, 1997.

[10] Hoffman, E., B. Warneke, E. J. J. Kruglick, J. Weigold, K. S. J. Pister, "3D Structures with Piezoresistive Standard CMOS," *Proceedings IEEE MEMS-95 Workshop on Micro Electro Mechanical Systems*, Amsterdam, The Netherlands, January 29 - February 2, pp. 288 - 293, 1995.

[11] FEI Company, 7451 NW Evergreen Parkway Hillsboro,OR 97124 USA. http://www.feic.com/main.htm

[12] W. C. Tang, T. C. H. Nguyen, R. T. Howe, "Laterally Driven Polysilicon Resonant Microstructures," *Sensors and Actuators (A)*, vol. 20, pp. 25 - 32, 1989.

[13] R. A. Lawton, M. Abraham, E. Lawrence, "Characterization of Non-planar Motion in MEMS Involving Scanning Laser Interferometry," *Proceedings SPIE*, vol. 3880, Santa Clara, California, pp. 46 - 50, September 20 - 22, 1999.

[14] Elite Engineering Corporation, 667 Rancho Conejo Road, Newbury Park, CA 91320 USA. http://www.eliteeng.com/

[15] G. Lin, K. S. J. Pister, and K. P. Roos, "Surface Micromachined Polysilicon Heart Cell Force Transducer," *Journal of Microelectromechanical Systems*, vol. 9, March 2000 (in press).

[16] Glass standard 0.75mm × 0.4mm × 6", catalog #6255, A-M Systems Inc., Everett, WA 98204 USA.

[17] P. A. Hofmann, and J. H. Lange, "Effects of Phosphorylation of Troponin I and C Protein on Isometric Tension and Velocity of Unloaded Shortening in Skinned Single Cardiac Myocytes From Rats," *Circulation Research*, vol. 74, no. 4, pp. 718 - 726, April 1994.

[18] R. E. Palmer, A. J. Brady, K. P. Roos, "Mechanical Measurements from Isolated Cardiac Myocytes Using a Pipette Attachment System," *Am. J. Physiol. 270 (Cell Physiol. 39)*: C697-C704, 1996.

[19] G. Lin, R. E. Palmer, K. S. J. Pister, and K. P. Roos, "Single Heart Cell Force Measured in Standard CMOS," *Transducers '97*, Chicago, Illinois, pp. 199 - 200, June 16 - 19, 1997.

[20] G. Lin, "MEMS Force Transducer System for Cellular Force Measurements," PhD Dissertation, UCLA Department of Electrical Engineering, School of Engineering and Applied Science, March 1998.